Brain Structure and Function (2019) 224:2045–2059
https://doi.org/10.1007/s00429-019-01892-y

ORIGINAL ARTICLE

Role of the insula in top–down processing: an intracranial EEG study using a visual oddball detection paradigm

Daphné Citherlet[1,2] · Olivier Boucher[1,3,4] · Julie Tremblay[5] · Manon Robert[1] · Anne Gallagher[3,5] · Alain Bouthillier[6] · Franco Lepore[3] · Dang Khoa Nguyen[1,2,7]

Received: 5 March 2018 / Accepted: 16 May 2019 / Published online: 25 May 2019

Abstract

Functional neuroimaging studies suggest that the insular cortex—and more especially the anterior insula (aI)—is involved in attentional processes and plays a crucial role in the "salience network". However, its specific role in attentional processing remains unclear, which is partly attributable to the low temporal resolution of non-invasive neuroimaging techniques. This study aims to examine the spatio-temporal dynamics of visual target processing using intracranial EEG recorded directly from the insula. Eight epileptic patients (four women, age 18–44 years) completed a three-stimulus visual oddball task during the extraoperative invasive intracranial EEG (iEEG) monitoring of their drug-resistant seizures. Depth electrodes were implanted in ten insular lobes (5 left and 5 right) and provided a total of 59 recording contacts in the insula. Event-related potentials (ERPs) and high-gamma-band responses (GBRs) were processed offline. Permutation analyses were performed to compare ERP signals across conditions during the P300 (225–400) interval, and modulations of GBRs (70−150 Hz) were computed for separate 100 ms time windows (from 0 to 1000 ms post-stimulus) and compared across conditions using non-parametric Wilcoxon test. Target stimuli were associated with a P300 (250–338 ms) component for 39% of contacts implanted in the aI, most probably reflecting voluntary attentional processing. Amplitude was significantly greater for target than for standard stimuli for all of these contacts, and was greater than for novel stimuli for 72%. In the posterior insula (pI), 16% of contacts showed preferential responses to target stimulus in the P300 interval. Increased GBRs in response to targets were observed in 53% of aI contacts (from ≈ 200 to 300 ms) and in 43% of pI contacts (from ≈ 400 to 500 ms). This study is the first to characterize the spatio-temporal dynamics of visual target processing in the insula using iEEG. Results suggest that visual targets elicit a P300 in the aI which corresponds in latency to the P3b component, suggesting that this region is involved in top–down processing of task-relevant information. GBRs to visual targets occur earlier in the aI than in the pI, further characterizing their respective roles in voluntary attentional processing.

Keywords Attention · Insula · Intracranial EEG · Orienting response · P300 · High gamma · Salience network · Target · Top–down · Visual oddball

✉ Dang Khoa Nguyen
d.nguyen@umontreal.ca

[1] Centre de Recherche du Centre Hospitalier de l'Université de Montreal (CHUM), Montreal, QC, Canada

[2] Département de Neurosciences, Université de Montréal, Montreal, Canada

[3] Département de Psychologie, Université de Montréal, Montreal, Canada

[4] Service de Psychologie, CHUM, Montreal, QC, Canada

[5] Centre de Recherche du CHU Sainte-Justine, Montreal, Canada

[6] Service de Neurochirurgie, CHUM, Montreal, QC, Canada

[7] Service de Neurologie, CHUM, 900 rue Saint-Denis, Montreal, QC H2X 0A9, Canada

Introduction

The insula (Island of Reil) is considered as the fifth lobe of the brain. This paralimbic structure is localized deep in the Sylvian fissure, enclosed by the frontal, parietal, and temporal opercula. It is divided into two portions by the central insular sulcus: the anterior insula (aI) and the posterior insula (pI). The aI is composed of three short gyri (anterior, middle, and posterior short gyri), and the pI is made of two long gyri (anterior and posterior long gyri) (Türe et al. 1999). The insula has been associated with a large variety of functions, including sensory (visceral, somatosensory, auditory, gustatory, and olfactory), affective (emotions and empathy), and cognitive (language, attention, and decision-making) processing (Uddin et al. 2017). It has also been proposed to be involved in autonomic and vestibular functions (Mazzola et al. 2014; Oppenheimer et al. 1992) and might be crucial for interoception (Craig 2003). However, its specific role(s) remain(s) enigmatic, which is partly attributable to its location which makes it difficult to access, and to the very rare prevalence of brain damage restricted to the insular cortex (Cereda et al. 2002).

Functional neuroimaging studies have revealed a functional differentiation within the insular lobe, with the aI being activated during cognitive and socio-emotional tasks, and the pI, by sensorimotor and chemosensory stimuli. More specifically, results from a meta-analysis of 1768 neuroimaging studies suggest that the anterior–dorsal region of the insula is activated during tasks assessing attention and working memory (Kurth et al. 2010). Indeed, activation of the aI has been reported in response to multimodal target detection and during goal-directed tasks (Clark et al. 2000; Downar et al. 2000; Kiehl et al. 2001; Linden et al. 1999; Nelson et al. 2010; Stevens et al. 2000). It has been suggested that the insular cortex is involved, along with other brain areas (e.g., supramarginal gyrus, frontal operculum, superior parietal lobule, and anterior cingulate cortex) in a "target detection network" which is used in the detection of visual target stimuli (Ardekani et al. 2002; Clark et al. 2000). More recently, the aI, along with the dorsal anterior cingulate cortex and subcortical and limbic structures, has been put in the core of the "salience network", which enables the attentional focus on the most salient stimuli in the environment (Menon and Uddin 2010; Uddin 2015). Currently, it remains unclear whether the aI participates in the voluntary (top–down) or automatic (bottom–up) detection of salient information, or in both processes.

Electroencephalography (EEG) studies have showed that the automatic and the voluntary/controlled processes involved in change detection can be distinguished both temporally and spatially. On scalp EEG, detection of an attended and unpredictable target stimulus is associated with an event-related potential (ERP) component peaking around 300–400 ms post-stimulus and maximal over the centro-parietal region. This positive-amplitude component, referred to as the P3b, reflects deliberate attentional processing for a relevant and expected stimulus. By contrast, novel task-irrelevant stimuli are associated with the P3a, which occurs 225–300 ms post-stimulus and maximal in the frontal region (Ardekani et al. 2002; Polich 2007; Posner et al. 1980; Snyder and Hillyard 1976; Squires et al. 1975). The P3b subcomponent occurs independently of the modality and tends to occur later in response to visual compared to auditory targets (Snyder et al. 1980). Both the P3a and the P3b components can be elicited during an oddball detection paradigm. Several electrophysiological studies using electrical sources localization by low-resolution electromagnetic tomography (LORETA) have helped characterizing the scalp topography and cortical sources of the P300 subcomponents. According to these studies, generators of the P3b include the insula, the temporal–parietal junction, the superior temporal gyrus, the dorsolateral prefrontal cortex (Mulert et al. 2004), the temporo-occipital regions, and the limbic as well as the anterior cingulate region (Volpe et al. 2007), whereas the generators of P3a are localized in cingulate region, frontal and right parietal areas (Volpe et al. 2007). A few studies using invasive intracranial EEG (iEEG) recordings with epileptic patients have showed P3a ERP responses to deviant stimuli located along the cingulate gyrus, the inferior frontal sulcus, the temporo-parietal cortex, the inferior temporal gyrus, and the posterior parahippocampus, and P3b ERP responses in the hippocampus, superior temporal sulcus, ventrolateral prefrontal cortex, and intraparietal sulcus (Baudena et al. 1995; Halgren et al. 1995a, b, 1998). To our knowledge, no study has yet described P3a or P3b components in the insula, which may be attributed to rare and/or incomplete sampling of this region in these studies.

Beyond its higher localization value, one major advantage of intracranial over scalp-EEG recording is the ability to measure signals in high frequencies (Parvizi and Kastner 2018). Several studies have showed that high-frequency (> 40 Hz) iEEG activity allows the investigation of task-related neural processes with high anatomical, temporal, and functional specificity (e.g., Lachaux et al. 2012). Increased activity in the high-gamma-frequency range (60–150 Hz) has been observed during functional activities in a variety of sensory and cognitive functions including sensorimotor, auditory, visual, attentional processing, memory, learning, and language, in both sensory and non-sensory areas (Jensen et al. 2007; Lachaux et al. 2012; Ray et al. 2008; Ward 2003). More specifically, gamma-frequency modulation has been proposed to serve as a mechanism for active maintenance of

representations in working memory, underlying the neuronal substrate for directed attention (Jensen et al. 2007). A scalp-EEG study has showed that gamma-band frequency differed between target and non-target-stimuli processing during an auditory oddball task. A late oscillatory activity peaking at 37 Hz around 360 ms was observed only after target stimuli, suggesting gamma-band frequency involvement in voluntary attentional function (Gurtubay et al. 2001). In a subdural electrocorticography study in humans, high-gamma modulation (80–150 Hz) was described from around 400 ms after stimulus onset in sensory and prefrontal cortices during a selective attentional task (Ray et al. 2008). More recently, intracranial electroencephalography recordings in epileptic patients have showed a modulation of high-frequency activity (70–150 Hz) in response to affective information, linking high-gamma modulation to saliency information processing (Boucher et al. 2015). Currently, very few studies have reported a high-gamma modulation in the insular cortex linked to attentional processing (e.g., Müsch et al. 2014). To our knowledge, no study has yet evaluated the spatio-temporal dynamics of attentional processing in the high-gamma-frequency range within the insular cortex.

In recent years, the insula has been recognized as a possible seizure focus in a non-negligible proportion of epileptic patients (Isnard et al. 2004; Nguyen et al. 2009; Obaid et al. 2017). Because of the widespread connections that the insula shares with other brain areas (Ghaziri et al. 2017), insular seizures are difficult to diagnose as they can mimic other more common types of epilepsies such as mesial temporal lobe epilepsy and frontal lobe epilepsy. Therefore, invasive iEEG recordings are often required in patients undergoing epilepsy surgery for whom an insular focus is suspected (Surbeck et al. 2011). Intracranial EEG offers a unique opportunity to study the role of the insula in information processing, by combining the excellent temporal resolution of EEG with a spatial resolution comparable to that of functional magnetic resonance imaging (fMRI) (Lachaux et al. 2003). In the present study, we use iEEG to examine the spatio-temporal dynamics of information processing in the insular cortex. More especially, this study aims to determine whether the insula is involved in the controlled/voluntary detection of task-relevant information (top–down processing), in the automatic detection of new information (bottom–up processing), or both, and whether this differs across insular subregions.

Experimental procedure

Participants

Eight epileptic patients (four female; mean age = 30.6, range = 18–44 years, all right-handed) with drug-resistant seizures, hospitalized for long-term extraoperative invasive iEEG monitoring to better delineate their epileptic focus, were recruited for the present study. Testing occurred at least 3 days after intracranial electrode implantation. All patients gave their informed written consent to participate to the experiment. The study was approved by the CHUM ethics committee, and was conducted in accordance with the ethical standards laid down in the Declaration of Helsinki. Table 1 summarizes characteristics of the study participants. A total of 59 electrode contacts were implanted in ten insulae (5 left and 5 right).

Oddball task

A three-stimulus visual oddball detection paradigm was employed to study attentional processing in the insula. Patients were tested in their hospital room and seated

Table 1 Descriptive characteristics of the study participants

Pt. #	Gender	Age (years)	Age at first seizure (years)	Implanted regions	Total no. of recording contacts	No. of contacts for analysis	No. of contacts in the insula	Seizure focus
1	F	18	10	L (F, P, T, I)	116	113	6	L Anterior insula
2	M	22	10	L (P, T, I)	110	110	3	Not determined
3	M	23	11	L (F, T, I) and R (F, T, I)	113	101	11	Bitemporal (Hippocampus)
4	M	34	20	R (F, P, T, I)	116	110	4	R Frontal
5	F	32	30	L (F, T, P, I, O)	116	111	11	L temporo-insular
6	F	37	23	L (C, F, P, I) and R (C, F, P, I)	101	95	19	R Cingular cortex
7	F	35	21	R (F, I, T)	84	82	2	R Operculo-orbito-insular
8	M	44	12	R (F, I, T)	94	92	3	R Middle and inferior frontal gyri junction

R right, *L* left, *F* frontal, *I* insula, *P* parietal, *O* occipital, *T* temporal, *C* cingulate

approximately 57 cm from the computer screen. Participants were instructed to keep their gaze on a cross localized at the centre of the screen, and to press the space key on the keyboard as quickly as possible in response to the target stimulus (blue square, 8 × 8 cm, 15% probability), and not to press in response to the standard (red square, 8 × 8 cm, 70%) and novel (green square, 8 × 8 cm, 15%) stimuli. Each block contained 70 standard stimuli, 15 target stimuli, and 15 novel stimuli. The total task includes six blocks of 100 stimuli presented in a pseudorandomized order. Stimulus duration was 50 ms and was presented centrally on a black background. Inter-stimuli interval was fixed at 2000 ms. Participants were offered a short pause between each block. Visual stimuli were presented on a 17 in. display monitor using Presentation software v. 14.5 (neurobehavioral systems: http://www.neurobs.com).

iEEG recording and analyses

Intracranial EEG acquisition was performed at 2 kHz using a Stellate Harmonie audio–video-EEG monitoring system (Natus Medical, San Carlos, CA), by means of depth electrodes, subdural strips, and grid electrodes (Ad-tech medical instruments, Racine, WI), with one mastoid used as reference and the other used as ground.

A 3D reconstruction with Stellate Gridview software was performed on postimplantation MRIs for localization of electrode contacts. Stellate Gridview coordinates were transformed to Talairach coordinates to allow an automatic localization of contacts according to the Talairach Daemon atlas (Lancaster et al. 2000), for visualization purposes. The distribution of the insular electrode contacts from the eight patients is illustrated in Fig. 1. A total of 59 contacts in the insula were analyzed in the present study.

EEG data were analyzed offline using Brain Vision Analyzer 2.0.1 software (Brain Products, Munich, Germany). All signals were down-sampled offline to 500 Hz. A visual inspection of raw data was applied. Channels with artefacts due to noise and epileptic activity on the whole signal were removed from further analyses (36/850, 4.2%, see Table 1). Automatic artefact rejection (± 300 µV), maximal allowed voltage step (30–60 µV/ms), and manual inspection of the data were performed to remove epochs containing noise and epileptic activity. We excluded on average 9.63% (between 3.39 and 18.86%) of data for each subject. Trials with errors and with responses occurring before 200 ms or after 2.000 ms following target-stimulus presentation were excluded.

ERP analysis

Data were segmented (− 200 to 1000 ms post-stimulus onset) separately for target, standard, and novel stimuli, and a baseline correction was applied (− 200 ms). We used high- and low-pass filters at 0.1 and 30 Hz as usually applied for studying the P300 components (e.g., Demiralp et al. 2001; Guger et al. 2011; Lindín et al. 2004), with a 60 Hz notch filter to limit the influence of power-line noise present in North America. Automatic peak detection was used to measure P300 amplitude (most positive point between 225 and 400 ms post-stimulus interval) and P300 latency (relative to stimulus onset). Only the components in the P300 latency range (i.e., 225–400 ms) were considered for future analysis. Visual inspection of the averaged ERP data did not reveal any other obvious amplitude difference in the 0–1000 ms post-stimulus interval. More than 75% of trials per condition were kept for analyses on average. However, only 21% of novel, 68% of standard, and 54% of target trials were conserved for one patient (Pt. #6). To this fact, results for this participant have had to be interpreted with this limitation. This procedure was performed using Brain Vision Analyzer 2.0.1 software.

GBR analysis

Data were segmented (− 500 to 1500 ms post-stimulus onset) separately for target, standard, and novel stimuli. Continuous time–frequency analysis over each trial was performed using complex Gaussian Morlet's wavelet in the frequency range of 70–150 Hz, in eight separate 10 Hz linear

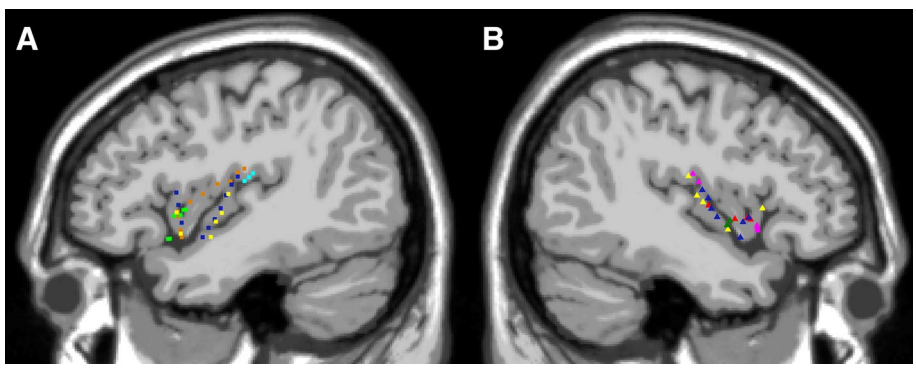

Fig. 1 Distribution of insular electrode contacts in our study participants ($N = 8$) according to the estimated Talairach coordinates, for the left (**a**) and right (**b**) hemispheres. Different colors were used to represent each patient: Pt. 1: green; Pt. 2: cyan; Pt. 3: yellow; Pt. 4: red; Pt. 5: brown; Pt. 6: blue; Pt. 7: dark green; Pt. 8: magenta

steps. The Morlet parameter was set at seven. A baseline correction (−200 to −50) was applied. We decided to select this frequency band based on the previous works that used 70–150 Hz band frequency to study intracranial gamma-band responses (Boucher et al. 2015; Vidal et al. 2010). This procedure was performed using Brain Vision Analyzer 2.0.1 software.

Due to epileptic focus in the insula and several seizures during the testing, we excluded one subject (Pt. # 5) from GBR analysis to avoid skewing our results with high-gamma activity originating from epileptic discharges. We kept on average 72% of trials for each subject, except for one (Pt. # 6) for whom only 18% of novel, 26% of target, and 59% of standard trials were conserved. At this step, we decided to exclude these two subjects for GBR analyses.

A broadband 70–150 Hz gamma-band power was computed, using a normalization method described earlier (Boucher et al. 2015) allowing for correction of the power decrease of the signal with increasing frequency due to the fact that event-related GBRs are broadband (Lachaux et al. 2012). For the eight separate frequency bands (10 Hz each one, from 70–80 to 140–150 Hz), power value for a given time interval was divided by the median value, on the same frequency band, from all the prestimulus baseline epochs. Broadband activity was computed by calculating the average of those eight normalized frequency layers. Epochs with outliers value (> 3.29 SD from the mean) were excluded. This procedure was repeated for each time interval, including the baseline (−200 to −50 ms) and for every 100 ms intervals (from 0 to 1000 ms post-stimulus). These values obtained represent the mean broadband gamma power over a time interval of 100 ms duration, expressed as the percentage of power change relative to baseline level for each insular contact. This procedure was performed using MatLab software (R2015a).

Statistical analysis

ERPs

Non-parametric permutation tests (Galán et al. 1997) were performed (1000 permutations) using MatLab software (R2015a). Electrode contacts showing a significant ($p < 0.001$) amplitude difference between the 225–400 ms interval at the baseline following target and/or novel stimuli were first identified. Then, for each of these contacts, permutation tests were performed to test for amplitude difference in the 225–400 ms interval between each pair of condition (i.e., target vs. standard; novel vs. standard; target vs. novel). At this step, a $p < 0.05$ criterion was used. Bonferroni correction was applied to avoid spurious positive results due to number of comparisons being performed for each electrode. We divided the alpha value criterion by the number of comparisons (i.e., target vs. standard; novel vs. standard; target vs. novel). Thus, a $p < 0.017$ criterion was used for each contact.

GBRs

Electrode contacts showing a significant response ($p < 0.001$) in the high-gamma band associated with presentation of target and/or novel stimuli were identified using Wilcoxon signed-rank tests comparing gamma-band power during each post-stimulus time interval to that of the prestimulus baseline epoch (−200 to −50 ms) on the same trial. Then, for each significant GBR identified for target and/or novel condition (i.e., each post-stimulus 100 ms time interval different from its baseline at the same contact), Mann–Whitney non-parametric tests were conducted to compare this GBR with each pair of condition (i.e., target vs. standard; novel vs. standard; target vs. novel). At this step, a $p < 0.05$ criterion was used. As previously, Bonferroni correction was applied for each contact ($p < 0.017$). All analyses were conducted in Matlab software (R2015a).

Results

Behavioral results

Performance on the visual oddball task is summarized in Table 2. The task was well executed by all patients, as all of them responded to more than 75% of targets and to ≤ 1% of non-targets. Mean reaction time differed strongly across participants. Patients who had slower hit reaction times (i.e., Pts. # 6 and 7) were also those with the lower hit detection rates.

Table 2 Behavioral results on the visual oddball task

Pt. #	No. blocks completed (/6)	% hits	% false alarms	Mean ± SD hit RT (ms)
1	5	100.0	0.0	448 ± 66
2	6	98.9	0.0	412 ± 57
3	6	98.9	1.1	444 ± 78
4	6	100.0	0.0	395 ± 40
5	6	100.0	0.0	297 ± 34
6	4	76.7	0.0	537 ± 128
7	4	83.3	0.0	553 ± 141
8	6	95.6	0.0	434 ± 67

Table 3 P300 (225–400 ms) responses to visual target recorded in the insular cortex

Pt. #	Anterior insula						Posterior insula					
	Contact	Hemisphere	Gyrus	P300 latency (ms)	P300 amplitude (μV)	Comparison	Contact	Hemisphere	Gyrus	P300 latency (ms)	P300 amplitude (μV)	Comparison
1	u11	Left	as-aps	338	+ 60	T > S*; T > N*						
	u12	Left	as	–	–	–						
	u13	Left	as	–	–	–						
	u31	Left	as	330	47.54	T > S*; T > N*						
	u32	Left	as	332	52.36	T > S*; T > N**						
	u52	Left	as	–	–	–						
2							u32	Left	al	326	19.17	T > N**
							u33	Left	al	326	29.51	T > S*; T > N*
							u34	Left	al	326	23.33	T > S*; T > N*
3	u11	Left	as-ia	284	20.94	T > S*; T > N**	u31	Left	pcs	–	–	–
	u12	Left	as	252	31.55	T > S*	u32	Left	pcs	–	–	–
	u21	Right	as-ms	270	16.35	T > S**; T > N**	u33	Left	al	–	–	–
							u34	Left	al	–	–	–
							u41	Right	al	–	–	–
							u42	Right	al	–	–	–
							u43	Right	al	–	–	–
							u44	Right	al	–	–	–
4	u22	Right	as	260	23.71	T > S*; T > N*	u42	Right	pl	276	14.50	n.s
	u23	Right	as	252	22.41	T > S*; T > N**						
	u24	Right	as	250	39.77	T > S*; T > N**						
5	u13	Left	as	–	–	–	u31	Left	al	–	–	–
	u14	Left	as	–	–	–	u32	Left	al	–	–	–
	u15	Left	as	–	–	–	u33	Left	al	–	–	–
	u16	Left	as	–	–	–	u34	Left	pl	–	–	–
	u17	Left	as	–	–	–						
	u35	Left	ms	–	–	–						
	u36	Left	as	–	–	–						
6	u11	Left	sis	–	–	–	u31	Left	cs	–	–	–
	u12	Left	ms-sis	298	36.89	T > S*	u32	Left	cs-li	304	28.30	T > S**
	u13	Left	ms-sis	–	–	–	u33	Left	al	–	–	–
	u21	Right	as-ia	298	39.41	T > S**	u34	Left	al	–	–	–
	u22	Right	ms-sis	–	–	–	u35	Left	al	–	–	–
	u23	Right	ms-sis	–	–	–	u36	Left	al	–	–	–
							u37	Left	al	–	–	–
							u41	Right	al	–	–	–
							u42	Right	al	–	–	–

Table 3 (continued)

Pt. #	Anterior insula						Posterior insula					
	Contact	Hemisphere	Gyrus	P300 latency (ms)	P300 amplitude (μV)	Comparison	Contact	Hemisphere	Gyrus	P300 latency (ms)	P300 amplitude (μV)	Comparison
							u43	Right	al	–	–	–
							u44	Right	al	–	–	–
							u45	Right	al	–	–	–
							u46	Right	al	–	–	–
7							u41	Right	al	–	–	–
							u42	Right	al	–	–	–
8	u22	Right	as	–	–	–						
	u23	Right	as	–	–	–						
	u24	Right	as	–	–	–						

Waveforms showing no significant activity in the P300 interval in comparison to baseline are identified with a '–' sign

T = Target; S = Standard; N = Novel; n.s = non significant; as = anterior short insular gyrus; aps = anterior peri-insular sulcus; al = anterior long insular gyrus; ms = middle short insular gyrus; ps = posterior short insular gyrus; pl = posterior long insular gyrus; ia = insular apex; pcs = post-central sulcus; sis = short insular sulcus; cs = central sulcus of the insula; li = limen insulae

*p value < 0.001

**p value < 0.01

iEEG results

ERPs

Target stimuli elicited a P300 response for 11/28 of aI contacts (39%) (i.e., 4/6 patients with aI contacts) (Pt. # 1, 3 contacts; Pt. # 3, 3 contacts; Pt. # 4, 3 contacts; and Pt. # 6, 2 contacts, see Table 3). Amplitude was significantly greater for targets than for standard stimuli for all of these contacts (100%), and was significantly greater than for novel stimuli for 8/11 contacts (72%) (Pt. # 1, 3 contacts; Pt. # 3, 2 contacts; and Pt. # 4, 3 contacts). Significant responses to target stimuli were observed at left (6/18, 33%) and at right (5/10, 50%) anterior insular electrode contacts. In patients with bilateral insular coverage, P300 latency was comparable for left and right aI contacts.

By contrast to aI responses, target stimuli elicited significant P300 responses in only 5/31 of pI contacts (16%) (Pt. # 2, 3 contacts; Pt. # 4, 1 contact; Pt. # 6, 1 contact). Amplitude was significantly greater for targets than for standard stimuli for 3/5 contacts (60%) (Pt. # 2, 2 contacts and Pt. # 6, 1 contact), and was significantly greater than for novel stimuli for 3/5 contacts (60%) (Pt. # 2, 3 contacts). All of these contacts were localized in the left hemisphere. The distribution of significant insular electrode contacts from the eight patients is illustrated in Fig. 2, and examples of P300 component recorded in the aI, and the grand average ERP for all aI contacts showing a significant P300 effect in response to target stimuli in the aI, are illustrated in Fig. 3.

Unlike target stimuli, novel (non-deviant target) stimuli did not elicit a significant P300 response in the insular cortex (see Table 4).

GBRs

In total, 8/15 aI contacts (53%) showed GBRs to target stimulus (Table 5). An early- and long-lasting (≈200–300 to 700 ms) target-dependent modulation of GBR was first observed for 7/15 of aI contacts (47%) (i.e., 4/4 patients with aI contacts) (Pt. # 1, 1 contact; Pt. # 3, 1 contacts; Pt. # 4, 3 contacts; and Pt. # 8, 2 contacts). More specifically, target-stimulus presentation was associated with increased GBRs in comparison to both standard and novel stimuli for all of these contacts (100%). A late- and short-lasting (from 600 to 700 ms) target-dependent modulation of GBRs was also recorded in one aI contact (1/15, Pt. # 8). Significant responses to target stimuli were observed at left (2/8, 25%) and at right (6/7, 86%) anterior insular contacts.

A later (≈400–500) modulation of gamma-band activity was observed in the pI in response to target stimulus for 5/14 contacts (36%) (i.e., 2/4 patients with pI contacts) (Pt. # 2, 3 contacts and Pt. # 3, 2 contacts). Target stimulus was associated with increased high-gamma activity in comparison

to both standard and novel stimuli for all of these contacts (100%) exclusively located in the left hemisphere. An early- and long-lasting (from 200 to 900 ms) target-dependent modulation of GBRs was recorded in one pI contact (1/14, Pt. # 4). In total, 6/14 pI contacts (43%) showed GBRs to target stimulus (Table 5).

Three aI contacts out of fifteen (20%) showed a novel-dependent modulation of GBRs (i.e., 2/4 patients with aI contacts) (Pt. # 4, 2 contacts and Pt. # 8, 1 contact). For each of these contacts, high-gamma power was stronger for novel than standard stimuli (see Table 6). Significant responses to novel stimuli were exclusively located in the right hemisphere.

Figure 4 depicts the distribution of insular contacts showing significant stimulus-dependent gamma-band modulations (A), along with the examples of GBRs recorded in the aI (B) and pI (C).

Discussion

This study examined the contribution of the human insula to visual target-stimulus detection, using iEEG recordings in epileptic patients. A significant proportion (39%) of aI contacts showed a significant ERP response following target stimuli occurring around 300 ms post-stimulus, most of which showed significantly greater response to targets than to both standard and novel stimuli, presumably reflecting a voluntary and controlled attention (i.e., top-down) effect. The results highlight the participation of the aI in the genesis of the P3b subcomponent, and also support an aI involvement in target detection as previously suggested by fMRI (Ardekani et al. 2002; Nelson et al. 2010) and scalp-EEG studies (Linden et al. 1999; Milner et al. 2014; Mulert et al. 2004). By contrast, a weak proportion (16%) of pI contacts responded preferentially to visual target stimuli, a result which is congruent with the functional differentiation within the insula as revealed by the previous studies (e.g., Kurth et al. 2010). A high proportion of aI contacts (53%) also showed early modulations of high-frequency signal in response to target stimuli, which highlights a top–down processing as previously suggested by an iEEG study (Müsch et al. 2014). Contrarily to our expectations, a significant proportion (43%) of pI contacts also showed GBRs to target stimulus starting around 400 ms. To our knowledge, our study is the first to characterize the P300 component and associated high-gamma modulations in the human insula using iEEG.

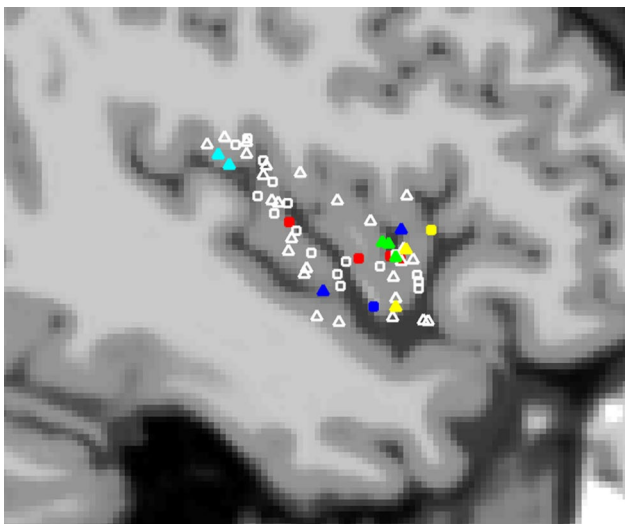

Fig. 2 Distribution of the insular electrode contacts showing a significant increase in P300 amplitude in response to target vs. standard and/or novel stimuli (both hemispheres combined). Different colors were used to represent each patient: Pt. 1: green; Pt. 2: cyan; Pt. 3: yellow; Pt. 4: red; Pt. 6: blue. White color: non significant insular electrode contacts

Brázdil et al. (2005) recorded intracerebral ERPs during a two-stimulus auditory oddball task in eight epileptic patients. Among the 606 intracerebral electrode sites investigated, only one was located in the insula, and although a "positive observation" was reported by the authors, there was no further information on the specific timing and location of this response. Clarke et al. (1999) reported a late, post-response, negative-going slow-wave component at insular/opercular electrode sites following rare targets in six patients, but no P3-like component during a visual oddball procedure. However, insular contacts in their study appeared to be located exclusively in the pI. Boucher et al. (2015) did not find GBRs in the insular cortex to saliency information processing. However, their patients with insular contacts had the seizure focus localized in the insula. A recent iEEG study has reported gamma-band oscillations (40–90 Hz) in the insula following thermo-nociceptive stimuli presentation (Liberati et al. 2017). The authors reported the role of the insula in the perceptual processing. However, no distinction between aI and pI in deeper attentional processing was investigated in the high-gamma frequency.

We observed P300 responses in both the left and the right insulae, with no obvious difference in latency and amplitude, as described in some neuroimaging studies (e.g., Linden et al. 1999). Other authors have previously showed a predominance of the right side for visual target-stimuli detection (e.g., Downar et al. 2000). Uddin (2015) proposed that an anomalous interaction between the right dorsal aI and other large-scale brain networks (i.e., the default-mode network and central executive network) could result in altered attentional processes, suggesting a key role of the right dorsal aI in salience processing. Our ERP results do not support such precedence for the right over the left insula in the attentional processes under study. Nevertheless, we cannot exclude the possibility that laterality-dependent effects

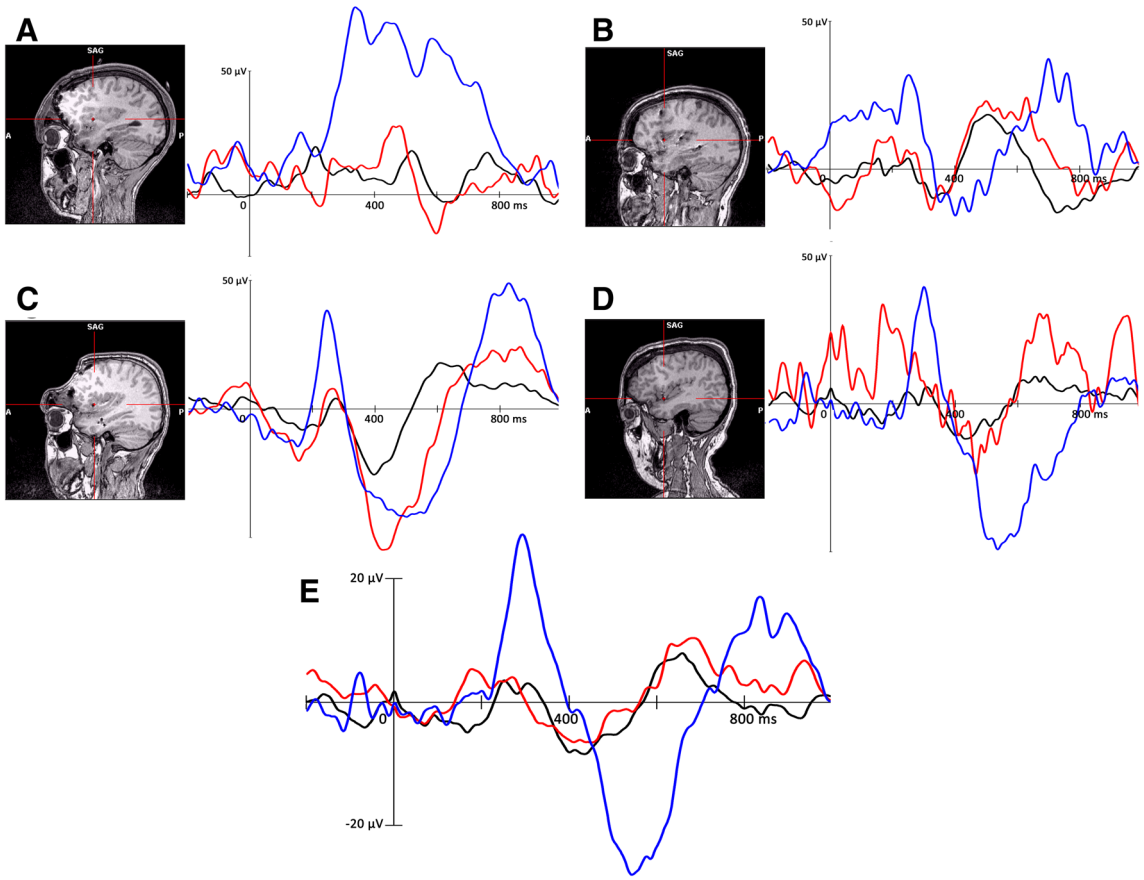

Fig. 3 Examples of P300 component recorded in the aI. **a** = Pt. 1, **b** = Pt. 3, **c** = Pt. 4, **d** = Pt. 6, and **e** = Grand average ERP for all aI contacts showing a significant P300 effect for target vs. standard stimuli. All significant contacts for a given participant were averaged prior to perform the grand average analysis, so that each participant has the same weight in the resulting ERP (blue: target, red: novel, and dark: standard)

would be observed in response to affective stimuli. Indeed, several lesion studies have highlighted the crucial participation of the right aI in the emotional processing (Phillips et al. 1997; Terasawa et al. 2015), and Paulus et al. (2003) have also showed a specific activation of the right aI following aversive stimuli presentation.

Out of six patients with electrode contacts in the aI, two (Pt's #5 and #8) did not show a significant P300 response. For one of them (Pt. #5), a left insular dysplasia was found on the MRI, and a left temporo-insular epileptic focus was identified, which might explain the lack of effect observed. This same patient was excluded from GBR analyses due to noise associated with inter-ictal high-frequency activity. The other patient (Pt. #8) had a right frontal cortical dysplasia (type II) and, although the insula was not found to be involved in the epileptic seizure genesis, we cannot exclude some cortical reorganization affecting the insula due to the dysplasia (Burneo et al. 2004; Gondo et al. 2000). By contrast to ERP analyses, we recorded GBRs in all aI contacts during target detection for these patients (Pt. #8). These seemingly contradictory findings illustrate how ERP and GBR analyses may offer complementary information. Indeed, P300 ERP responses mostly reflect theta and delta frequency activities (Bernat et al. 2007; Kolev et al. 1997).

In one patient (Pt. #6), the P3b recorded in the three aI contacts for target stimuli differed from the standard stimuli, but did not differ significantly from the novel stimuli. This may be attributable to the low number of novel trials for these three contacts (21%) kept for analysis after artefact rejection compared to target stimuli (53%) in this subject (significant statistical comparison (t (3) = − 11.58, p = 0.007), thereby affecting statistical power for target vs. novel stimuli in this patient. We did not find aI contacts with P300 activity in response to novel stimuli in comparison to standard stimuli, and only 3/15 aI contacts showed GBRs for this comparison. Thus, the aI does not seem to respond preferentially to rare stimuli, but rather to task-relevant stimuli, suggesting a top-down effect related to attentional control (Clark et al. 2000; Nelson et al. 2010). The aI plays a major role in affective processing including emotional evaluation, social cognition, empathy, and consciousness emotional (e.g., Berntson et al. 2011). Furthermore, Menon

Table 4 P300 (225–400 ms) responses to novel stimuli in the insular cortex

Pt. #	Anterior insula						Posterior insula					
	Contact	Hemisphere	Gyrus	P300 latency	P300 amplitude	Comparison	Contact	Hemisphere	Gyrus	P300 latency	P300 amplitude	Comparison
1	u11	Left	as-aps	–	–	–						
	u12	Left	as	–	–	–						
	u13	Left	as	–	–	–						
	u31	Left	as	–	–	–						
	u32	Left	as	–	–	–						
	u52	Left	as	–	–	–						
2							u32	Left	al	–	–	–
							u33	Left	al	–	–	–
							u34	Left	al	–	–	–
3	u11	Left	as-ia	–	–	–	u31	Left	pcs	–	–	–
	u12	Left	as	–	–	–	u32	Left	pcs	–	–	–
	u21	Right	as-ms	–	–	–	u33	Left	al	–	–	–
							u34	Left	al	–	–	–
							u41	Right	al	–	–	–
							u42	Right	al	–	–	–
							u43	Right	al	–	–	–
							u44	Right	al	–	–	–
4	u22	Right	as	–	–	–	u42	Right	pl	–	–	–
	u23	Right	as	–	–	–						
	u24	Right	as	–	–	–						
5	u13	Left	as	–	–	–	u31	Left	al	–	–	–
	u14	Left	as	–	–	–	u32	Left	al	–	–	–
	u15	Left	as	–	–	–	u33	Left	al	–	–	–
	u16	Left	as	–	–	–	u34	Left	pl	–	–	–
	u17	Left	as	–	–	–						
	u35	Left	ms	–	–	–						
	u36	Left	as	–	–	–						
6	u11	Left	sis	–	–	–	u31	Left	cs	–	–	–
	u12	Left	ms-sis	–	–	–	u32	Left	cs-li	–	–	–
	u13	Left	ms-sis	–	–	–	u33	Left	al	–	–	–
	u21	Right	as-ia	–	–	–	u34	Left	al	–	–	–
	u22	Right	ms-sis	–	–	–	u35	Left	al	–	–	–
	u23	Right	ms-sis	–	–	–	u36	Left	al	–	–	–
							u37	Left	al	–	–	–
							u41	Right	al	–	–	–
							u42	Right	al	–	–	–

Table 4 (continued)

Pt. #	Anterior insula						Posterior insula					
	Contact	Hemisphere	Gyrus	P300 latency	P300 amplitude	Comparison	Contact	Hemisphere	Gyrus	P300 latency	P300 amplitude	Comparison
							u43	Right	al	–	–	–
							u44	Right	al	–	–	–
							u45	Right	al	–	–	–
							u46	Right	al	–	–	–
7							u41	Right	al	–	–	–
							u42	Right	al	–	–	–
8	u22	Right	as	–	–	–						
	u23	Right	as	–	–	–						
	u24	Right	as	–	–	–						

Waveforms showing no significant activity in the P300 interval in comparison to baseline are identified with a '–' sign

T = Target; S = Standard; N = Novel; n.s = non significant; as = anterior short insular gyrus; aps = anterior peri-insular sulcus; al = anterior long insular gyrus; ms = middle short insular gyrus; ps = posterior short insular gyrus; pl = posterior long insular gyrus; ia = insular apex; pcs = post-central sulcus; sis = short insular sulcus; cs = central sulcus of the insula; li = limen insulae

and Uddin (2010) have proposed that the aI would help to integrate bottom–up salient information in initiating attentional control signal. As the stimuli involved in our task were emotionally neutral, we cannot exclude the possibility that the aI is involved in bottom–up detection of task irrelevant, but emotionally relevant novel stimuli (Britton et al. 2006; Phan et al. 2004; Zhang et al. 2018).

One patient (Pt. #2) showed significant P300 responses in the pI for target-stimuli detection around 326 ms post-stimuli, which was not seen in the other participants. Although these inter-individual differences may be attributable to differences in the specific locations of the insular contacts or to the fact that contacts may not have all been implanted in the same cortical layer, this may also reflect inter-individual differences in anatomo-functional organization of the insular cortex, possibly due to plasticity (Scharfman 2002). This patient also showed GBRs in the pI for target stimuli in comparison to novel and standard stimuli around 400–600 ms post-stimuli.

Together, ERP and GBRs results for the aI contacts showed that this insular subportion is involved in top-down attentional processing. Contrary to our expectations, several pI contacts showed a later target-dependent modulation of GBRs in comparison to novel and standard stimuli presentation. Rather than indexing attentional processing, this activity may reflect somatosensory or motor responses associated with target responding, which would be congruent with the role of the pI in sensorimotor processing (Cauda et al. 2011; Kishima et al. 2007; Nguyen et al. 2009). This hypothesis is supported by the fact that pI contacts showing these relatively late GBRs were all localized in the left hemisphere, while all participants pressed the response button using the right hand. Future studies using similar paradigms should use non-motor responses (e.g., counting the targets) to rule out the possibility that the recorded pI activity is attributable to such processes.

This study is limited by factors that are inherent to iEEG studies with epileptic patients. These include the incomplete coverage of the insular cortex by intracranial electrodes, the limitation of generalization of our results due to the possible influence of epilepsy (especially in the three patients for whom the epileptic focus involved in insula) and cortical dysplasia on the functional organization of the insula, and the influence of medication on neural activity. Despite these limitations, our results are congruent across patients as well as with prior studies with healthy participants.

This study examined attentional processes in the insular cortex through direct intracranial EEG recordings by exploring ERP subcomponents and GBRs obtained during a three-stimulus visual oddball task. Our findings suggest that visual target detection is associated with a P300 response in the aI which seems to correspond to the P3b component seen in scalp-EEG studies, underlying voluntary attentional

Table 5 High-gamma modulations (70–150 Hz) in response to visual target recorded in the insular cortex

Pt. #	Anterior insula					Posterior insula				
	Contact	Hemisphere	Gyrus	Comparison	Timing (ms)	Contact	Hemisphere	Gyrus	Comparison	Timing (ms)
1	u11	Left	as-aps	–	–					
	u12	Left	as	–	–					
	u13	Left	as	–	–					
	u31	Left	as	–	–					
	u32	Left	as	–	–					
	u52	Left	as	T>S; T>N	400–600					
2						u32	Left	al	T>S; T>N	600–700
						u33	Left	al	T>S; T>N	400–700
						u34	Left	al	T>S; T>N	400–700
3	u11	Left	as-ia	T>S; T>N	200–300	u31	Left	pcs	–	–
	u12	Left	as	–	–	u32	Left	pcs	–	–
	u21	Right	as-ms	–	–	u33	Left	al	T>S; T>N	600–800
						u34	Left	al	T>S; T>N	500–1000
						u41	Right	al	–	–
						u42	Right	al	–	–
						u43	Right	al	–	–
						u44	Right	al	–	–
4	u22	Right	as	T>S; T>N	200–800	u42	Right	pl	T>S; T>N	200–900
	u23	Right	as	T>S; T>N	200–500					
	u24	Right	as	T>S; T>N	200–500					
7						u41	Right	al	–	–
						u42	Right	al	–	–
8	u22	Right	as	T>S; T>N	400–800					
	u23	Right	as	T>S; T>N	300–900					
	u24	Right	as	T>S; T>N	600–700					

All significant contacts showed a p value < 0.01

T = Target; S = Standard; N = Novel; as = anterior short insular gyrus; aps = anterior peri-insular sulcus; al = anterior long insular gyrus; ms = middle short insular gyrus; ps = posterior short insular gyrus; pl = posterior long insular gyrus; ia = insular apex; pcs = post-central sulcus; sis = short insular sulcus; cs = central sulcus of the insula; li = limen insulae

processing. This P300 response appeared to be independent from the hemisphere where recordings were obtained, and was not consistently observed in the pI. GBRs were also recorded in response to target stimuli, occurring earlier in the aI (from ≈ 200 to 300 ms) and then in the pI (from ≈ 400 to 500 ms). This temporal separation might reflect contribution of the aI to voluntary attentional processing, and the role of the pI in sensorimotor processing.

Table 6 High-gamma modulations (70–150 Hz) in response to novel stimuli in the insular cortex

Pt. #	Anterior insula					Posterior insula				
	Contact	Hemisphere	Gyrus	Comparison	Timing (ms)	Contact	Hemisphere	Gyrus	Comparison	Timing (ms)
1	u11	Left	as-aps	–	–					
	u12	Left	as	–	–					
	u13	Left	as	–	–					
	u31	Left	as	–	–					
	u32	Left	as	–	–					
	u52	Left	as	–	–					
2						u32	Left	al	–	–
						u33	Left	al	–	–
						u34	Left	al	–	–
3	u11	Left	as-ia	–	–	u31	Left	pcs	–	–
	u12	Left	as	–	–	u32	Left	pcs	–	–
	u21	Right	as-ms	–	–	u33	Left	al	–	–
						u34	Left	al	–	–
						u41	Right	al	–	–
						u42	Right	al	–	–
						u43	Right	al	–	–
						u44	Right	al	–	–
4	u22	Right	as	N > S	200–500	u42	Right	pl	–	–
	u23	Right	as	N > S	300–500					
	u24	Right	as	–	–					
7						u41	Right	al	–	–
						u42	Right	al	–	–
8	u22	Right	as	–	–					
	u23	Right	as	N > S	400–500					
	u24	Right	as	–	–					

All significant contacts showed a p value < 0.01

T = Target; S = Standard; N = Novel; as = anterior short insular gyrus; aps = anterior peri-insular sulcus; al = anterior long insular gyrus; ms = middle short insular gyrus; ps = posterior short insular gyrus; pl = posterior long insular gyrus; ia = insular apex; pcs = post-central sulcus; sis = short insular sulcus; cs = central sulcus of the insula; li = limen insulae

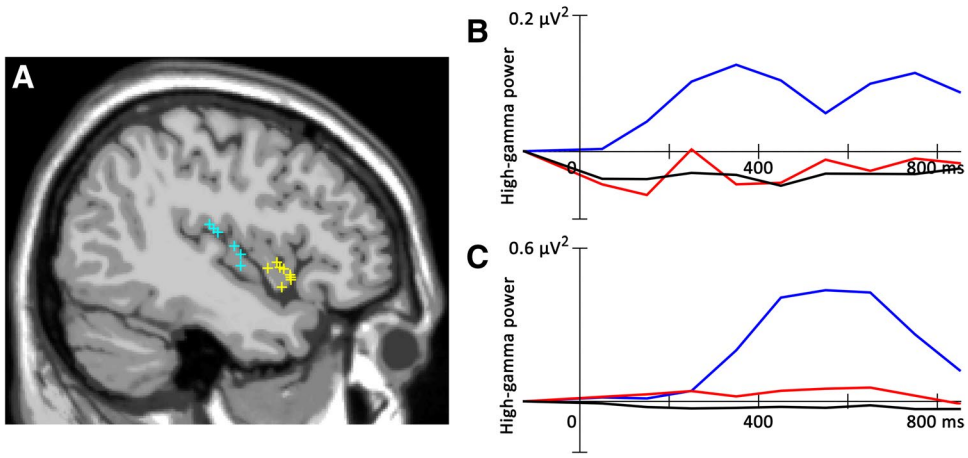

Fig. 4 Distribution of insular contacts showing significant high-gamma modulation in response to target stimuli (yellow: aI and blue: pI) (**a**) and the average of significant contacts showing high-gamma activity, relative to baseline, in the aI (**b**) and pI (**c**), across conditions (blue: target, red: novel, and dark: standard)

Funding Canadian Institutes of Health Research (CIHR)—Project Grant (148563-DKN, FL, OB); CIHR Postdoctoral Grant (MFE-115520–OB); Natural Sciences and Engineering Research Council of Canada (NSERC)—Discovery Grant (RGPIN-2016-05216-DKN, FL, KJ).

References

Ardekani BA, Choi SJ, Hossein-Zadeh GA, Porjesz B, Tanabe JL, Lim KO, Begleiter H (2002) Functional magnetic resonance imaging of brain activity in the visual oddball task. Cogn Brain Res 14(3):347–356

Baudena P, Halgren E, Heit G, Clarke JM (1995) Intracerebral potentials to rare target and distractor auditory and visual stimuli. III. Frontal cortex. Electroencephalogr Clin Neurophysiol 94(4):251–264

Bernat EM, Malone SM, Williams WJ, Patrick CJ, Iacono WG (2007) Decomposing delta, theta, and alpha time–frequency ERP activity from a visual oddball task using PCA. Int J Psychophysiol 64(1):62–74

Berntson GG, Norman GJ, Bechara A, Bruss J, Tranel D, Cacioppo JT (2011) The insula and evaluative processes. Psychol Sci 22(1):80–86

Boucher O, D'hondt F, Tremblay J, Lepore F, Lassonde M, Vannasing P et al (2015) Spatiotemporal dynamics of affective picture processing revealed by intracranial high-gamma modulations. Hum Brain Mapp 36(1):16–28

Brázdil M, Dobšík M, Mikl M, Hluštík P, Daniel P, Pažourková M et al (2005) Combined event-related fMRI and intracerebral ERP study of an auditory oddball task. Neuroimage 26(1):285–293

Britton JC, Taylor SF, Sudheimer KD, Liberzon I (2006) Facial expressions and complex IAPS pictures: common and differential networks. Neuroimage 31(2):906–919

Burneo JG, Kuzniecky RI, Bebin M, Knowlton RC (2004) Cortical reorganization in malformations of cortical development a magnetoencephalographic study. Neurology 63(10):1818–1824

Cauda F, D'agata F, Sacco K, Duca S, Geminiani G, Vercelli A (2011) Functional connectivity of the insula in the resting brain. Neuroimage 55(1):8–23

Cereda C, Ghika J, Maeder P, Bogousslavsky J (2002) Strokes restricted to the insular cortex. Neurology 59(12):1950–1955

Clark VP, Fannon S, Lai S, Benson R, Bauer L (2000) Responses to rare visual target and distractor stimuli using event-related fMRI. J Neurophysiol 83(5):3133–3139

Clarke JM, Halgren E, Chauvel P (1999) Intracranial ERPs in humans during a lateralized visual oddball task: II. Temporal, parietal, and frontal recordings. Clin Neurophysiol 110:1224–1225

Craig AD (2003) Interoception: the sense of the physiological condition of the body. Curr Opin Neurobiol 13(4):500–505

Demiralp T, Ademoglu A, Istefanopulos Y, Başar-Eroglu C, Başar E (2001) Wavelet analysis of oddball P300. Int J Psychophysiol 39(2–3):221–227

Downar J, Crawley AP, Mikulis DJ, Davis KD (2000) A multimodal cortical network for the detection of changes in the sensory environment. Nat Neurosci 3(3):277–283

Galán L, Biscay R, Rodríguez JL, Pérez-Abalo MC, Rodriguez R (1997) Testing topographic differences between event related brain potentials by using non-parametric combinations of permutation tests. Electroencephalogr Clin Neurophysiol 102(3):240–247

Ghaziri J, Tucholka A, Girard G, Houde JC, Boucher O, Gilbert G et al (2017) The corticocortical structural connectivity of the human insula. Cereb Cortex 27(2):1216–1228

Gondo K, Kira R, Tokunaga Y, Harashima C, Tobimatsu S, Yamamoto T, Hara T (2000) Reorganization of the primary somatosensory area in epilepsy associated with focal cortical dysplasia. Dev Med Child Neurol 42(12):839–842

Guger C, Edlinger G, Krausz G (2011) Hardware/software components and applications of BCIs. In: Fazel R (ed.) recent advances in brain-computer interface systems. ISBN: 978-953-307-175-6, InTech, Available from: https://www.intechopen.com/books/recent-advances-in-brain-computer-interface-systems/hardware-software-components-and-applications-of-bcis

Gurtubay IG, Alegre M, Labarga A, Malanda A, Iriarte J, Artieda J (2001) Gamma band activity in an auditory oddball paradigm studied with the wavelet transform. Clin Neurophysiol 112(7):1219–1228

Halgren E, Baudena P, Clarke JM, Heit G, Liégeois C, Chauvel P, Musolino A (1995a) Intracerebral potentials to rare target and distractor auditory and visual stimuli. I. Superior temporal plane and parietal lobe. Electroencephalogr Clin Neurophysiol 94(3):191–220

Halgren E, Baudena P, Clarke JM, Heit G, Marinkovic K, Devaux B et al (1995b) Intracerebral potentials to rare target and distractor auditory and visual stimuli. II. Medial, lateral and posterior temporal lobe. Electroencephalogr Clin Neurophysiol 94(4):229–250

Halgren E, Marinkovic K, Chauvel P (1998) Generators of the late cognitive potentials in auditory and visual oddball tasks. Electroencephalogr Clin Neurophysiol 106(2):156–164

Isnard J, Guénot M, Sindou M, Mauguiere F (2004) Clinical manifestations of insular lobe seizures: a stereo-electroencephalographic study. Epilepsia 45(9):1079–1090

Jensen O, Kaiser J, Lachaux JP (2007) Human gamma-frequency oscillations associated with attention and memory. Trends Neurosci 30(7):317–324

Kiehl KA, Laurens KR, Duty TL, Forster BB, Liddle PF (2001) Neural sources involved in auditory target detection and novelty processing: an event-related fMRI study. Psychophysiology 38(1):133–142

Kishima H, Saitoh Y, Osaki Y, Nishimura H, Kato A, Hatazawa J, Yoshimine T (2007) Motor cortex stimulation in patients with deafferentation pain: activation of the posterior insula and thalamus. J Neurosurg 107(1):43–48

Kolev V, Demiralp T, Yordanova J, Ademoglu A, Isoglu-Alkaç Ü (1997) Time–frequency analysis reveals multiple functional components during oddball P300. NeuroReport 8(8):2061–2065

Kurth F, Zilles K, Fox PT, Laird AR, Eickhoff SB (2010) A link between the systems: functional differentiation and integration within the human insula revealed by meta-analysis. Brain Struct Funct 214(5–6):519–534

Lachaux JP, Rudrauf D, Kahane P (2003) Intracranial EEG and human brain mapping. J Physiol Paris 97(4):613–628

Lachaux JP, Axmacher N, Mormann F, Halgren E, Crone NE (2012) High-frequency neural activity and human cognition: past, present and possible future of intracranial EEG research. Prog Neurobiol 98(3):279–301

Lancaster JL, Woldorff MG, Parsons LM, Liotti M, Freitas CS, Rainey L et al (2000) Automated Talairach atlas labels for functional brain mapping. Hum Brain Mapp 10(3):120–131

Liberati G, Klöcker A, Algoet M, Mulders D, Maia Safronova M, Ferrao Santos S et al (2017) Gamma-band oscillations preferential for nociception can be recorded in the human insula. Cereb Cortex 28(10):3650–3664

Linden DE, Prvulovic D, Formisano E, Völlinger M, Zanella FE, Goebel R, Dierks T (1999) The functional neuroanatomy of target detection: an fMRI study of visual and auditory oddball tasks. Cereb Cortex 9(8):815–823

Lindín M, Zurrón M, Díaz F (2004) Changes in P300 amplitude during an active standard auditory oddball task. Biol Psychol 66(2):153–167

Mazzola L, Lopez C, Faillenot I, Chouchou F, Mauguiere F, Isnard J (2014) Vestibular responses to direct stimulation of the human insular cortex. Ann Neurol 76(4):609–619

Menon V, Uddin LQ (2010) Saliency, switching, attention and control: a network model of insula function. Brain Struct Funct 214(5–6):655–667

Milner R, Rusiniak M, Lewandowska M, Wolak T, Ganc M, Piątkowska-Janko E et al (2014) Towards neural correlates of auditory stimulus processing: a simultaneous auditory evoked potentials and functional magnetic resonance study using an oddball paradigm. Med Sci Monit 20:35

Mulert C, Jäger L, Schmitt R, Bussfeld P, Pogarell O, Möller HJ et al (2004) Integration of fMRI and simultaneous EEG: towards a comprehensive understanding of localization and time-course of brain activity in target detection. Neuroimage 22(1):83–94

Müsch K, Hamamé CM, Perrone-Bertolotti M, Minotti L, Kahane P, Engel AK, Schneider TR (2014) Selective attention modulates high-frequency activity in the face-processing network. Cortex 60:34–51

Nelson SM, Dosenbach NU, Cohen AL, Wheeler ME, Schlaggar BL, Petersen SE (2010) Role of the anterior insula in task-level control and focal attention. Brain Struct Funct 214(5–6):669–680

Nguyen DK, Nguyen DB, Malak R, Leroux JM, Carmant L, Saint-Hilaire JM et al (2009) Revisiting the role of the insula in refractory partial epilepsy. Epilepsia 50(3):510–520

Obaid S, Zerouali Y, Nguyen DK (2017) Insular Epilepsy: Semiology and Noninvasive Investigations. J Clin Neurophysiol 34(4):315–323

Oppenheimer SM, Gelb A, Girvin JP, Hachinski VC (1992) Cardiovascular effects of human insular cortex stimulation. Neurology 42(9):1727

Parvizi J, Kastner S (2018) Promises and limitations of human intracranial electroencephalography. Nature Neuroscience 21(4):474–483

Paulus MP, Rogalsky C, Simmons A, Feinstein JS, Stein MB (2003) Increased activation in the right insula during risk-taking decision making is related to harm avoidance and neuroticism. Neuroimage 19(4):1439–1448

Phan KL, Taylor SF, Welsh RC, Ho SH, Britton JC, Liberzon I (2004) Neural correlates of individual ratings of emotional salience: a trial-related fMRI study. Neuroimage 21(2):768–780

Phillips ML, Young AW, Senior C, Brammer M, Andrew C, Calder AJ et al (1997) A specific neural substrate for perceiving facial expressions of disgust. Nature 389(6650):495

Polich J (2007) Updating P300: an integrative theory of P3a and P3b. Clin Neurophysiol 118(10):2128–2148

Posner MI, Snyder CR, Davidson BJ (1980) Attention and the detection of signals. J Exp Psychol Gen 109(2):160

Ray S, Niebur E, Hsiao SS, Sinai A, Crone NE (2008) High-frequency gamma activity (80–150 Hz) is increased in human cortex during selective attention. Clin Neurophysiol 119(1):116–133

Scharfman HE (2002) Epilepsy as an example of neural plasticity. The Neuroscientist 8(2):154–173

Snyder E, Hillyard SA (1976) Long-latency evoked potentials to irrelevant, deviant stimuli. Behavioral Biology 16(3):319–331

Snyder E, Hillyard SA, Galambos R (1980) Similarities and differences among the P3 waves to detected signals in three modalities. Psychophysiology 17(2):112–122

Squires NK, Squires KC, Hillyard SA (1975) Two varieties of long-latency positive waves evoked by unpredictable auditory stimuli in man. Electroencephalogr Clin Neurophysiol 38(4):387–401

Stevens AA, Skudlarski P, Gatenby JC, Gore JC (2000) Event-related fMRI of auditory and visual oddball tasks. Magn Reson Imaging 18(5):495–502

Surbeck W, Bouthillier A, Weil AG, Crevier L, Carmant L, Lortie A et al (2011) The combination of subdural and depth electrodes for intracranial EEG investigation of suspected insular (perisylvian) epilepsy. Epilepsia 52(3):458–466

Terasawa Y, Kurosaki Y, Ibata Y, Moriguchi Y, Umeda S (2015) Attenuated sensitivity to the emotions of others by insular lesion. Front Psychol 6:1314

Türe U, Yaşargil DC, Al-Mefty O, Yaşargil MG (1999) Topographic anatomy of the insular region. J Neurosurg 90(4):720–733

Uddin LQ (2015) Salience processing and insular cortical function and dysfunction. Nat Rev Neurosci 16(1):1–7

Uddin LQ, Nomi JS, Hébert-Seropian B, Ghaziri J, Boucher O (2017) Structure and function of the human insula. J Clin Neurophysiol 34(4):300–306

Vidal JR, Ossandón T, Jerbi K, Dalal SS, Minotti L, Ryvlin P et al (2010) Category-specific visual responses: an intracranial study comparing gamma, beta, alpha, and ERP response selectivity. Front Hum Neurosci 4:195

Volpe U, Mucci A, Bucci P, Merlotti E, Galderisi S, Maj M (2007) The cortical generators of P3a and P3b: a LORETA study. Brain Res Bull 73(4):220–230

Ward LM (2003) Synchronous neural oscillations and cognitive processes. Trends Cogn Sci 7(12):553–559

Zhang Y, Zhou W, Wang S, Zhou Q, Wang H, Zhang B et al (2018) The roles of subdivisions of human insula in emotion perception and auditory processing. Cereb Cortex 29(2):517–528